Synthesis and Characterization of Monodisperse Doped ZnS Nanospheres with Enhanced Thermal Stability

Yue Zhang and Yadong Li*

Department of Chemistry and the Key Laboratory of Atomic & Molecular Nanosciences (Ministry of Education, China), Tsinghua University, Beijing, 100084, P. R. China and National center for nanoscience and nanotechnology; Beijing, 100084, P. R. China

Received: June 14, 2004; In Final Form: September 8, 2004

The monodisperse ZnS nanospheres, with an average diameter of 100 nm, were synthesized through a solvothermal method. Strong photoluminescence emission from blue to green and orange can be observed by doping these ZnS nanospheres with various cations (Mn^{2+}, Cu^{2+}, Al^{3+}). An investigation is reported on the coating of ZnS nanospheres by a thin shell of SiO_2 or TiO_2 using a sol−gel process. X-ray diffraction (XRD), transmission electron microscopy (TEM), and energy dispersive spectroscopy (EDS) were used for the characterization of the coated ZnS nanospheres. The photoluminescence properties demonstrated that not only the brightness of the coated nanospheres has been enhanced but also the thermal stability has been improved greatly.

Introduction

Semiconductor nanoparticles have attracted widespread attention because of their special optical and electronic properties arising from the quantum confinement of electrons and large surface area. At this point, the optical properties of these semiconductor nanocrystals have been the prominent research focus. Among these semiconductor materials, zinc sulfide (ZnS), a band gap material with E_g of 3.66 eV at room temperature, shows various luminescence properties such as photoluminescence,[1−2] electroluminescence,[3] mechanoluminescence,[4] and thermal luminescence.[5] Therefore, ZnS is a traditional phosphor widely used in flat-panel display, electroluminescent devices, infrared windows, sensors, and lasers.[6−8] Doped ZnS with selected metal ions is a promising material in mechano-optic applications.[9] The photoluminescence of Cu, Co, Eu, Ce, and Er doped ZnS nanomaterials has also been investigated.[10−14] In general, the spherically monodisperse morphology is an important factor for the low-light scattering at the surfaces, as well as the high-packing densities.[15]

Up to now, many synthetic methods have been employed to prepare ZnS nanocrystals with various shapes.[16−25] To fully utilize the functional properties of the nanoparticles, well-dispersed systems are desirable. Recently, solvents and the soft templates have been widely used to control the synthesis of semiconductor nanomaterials because their coordination interaction with metal ions provides a good way to control the size and, more importantly, the size distribution of nanocrystals. By changing the reaction conditions, for example, the concentration of starting materials, the nature of the solvents, and the suitable capping/stabilizing agents, it is possible to synthesize a variety of nanocrystallites with different sizes. In the solvothermal process, the capping agent can covalently bind to the surface atoms of the nanocrystallite and can thus prevent them from forming bulk materials. Therefore, solvothermal process has recently been extensively applied to the synthesis and design of nanomaterials of new structures and properties.

* Author to whom correspondence should be addressed. E-mail: ydli@tsinghua.edu.cn.

However, during the operation, such sulfide phosphors degrade and disperse into the vacuum, contaminating the field emitter and thus hindering electron emission. To overcome this drawback, covering their surface with a shell to enhance the chemical stability of them is a frequently used technique. The coating compounds can differ in a wide range, such as large-band-gap semiconductor materials, polymers, or insulators such as silica, titania, and so forth.[26−29] In the meantime, the properties (optical, magnetic, and catalytic) of nanoparticles can be altered by coating too.[26,28,30−31] For photoluminescence properties, the shell has to be transparent, hard, and highly resistible to moisture and chemical deterioration. Besides, a homogeneous coating with the right amount outside the individual phosphors is also important, for the nonhomogeneous coating can lead to the formation of pockets that may have local excess or lack of coating materials. Such pockets can result in a nonuniform distribution of properties within the cores. Although many reports of the coated bulk ZnS can be found,[32−35] few of them are presented on the synthesis of ZnS nanopatricles. It is, moreover, advantageous to work with dispersed spherical materials to serve as cores in practical applications.

In this work, a novel solvothermal route to the preparation of monodisperse ZnS nanospheres is reported, which has many advantages in comparison with other methods.[23−25,36] It does not require organometallic or toxic precursors and can be carried out at the low temperatures. By employing a suitable capping agent and adjusting the reaction conditions, monodisperse ion-doped (Mn^{2+}, Cu^{2+}, Al^{3+}) ZnS nanospheres with homogeneous shape and size can be obtained. For the syntheses of coated ZnS nanospheres, SiO_2 and TiO_2 are used as the coating materials. Uniform particles of SiO_2 and TiO_2 have been synthesized by hydrolysis of alkoxides in alcohol solutions. Controlled hydrolysis can be achieved by appropriately adjusting the experimental parameters. The photoluminescence (PL) properties of doped and coated ZnS are investigated.

Experimental Section

A. Synthesis of Monodisperse Doped ZnS Nanospheres. The analytical grade regents of $ZnCl_2$, $MnCl_2$, $CuCl_2$, and $AlCl_3$

10.1021/jp047446c CCC: $27.50
Published on Web 10/22/2004

were used as starting materials. The doped ZnS nanospheres were synthesized similar to that in the previous report[37] in which oleic acid was used as the capping agent. In addition, dodecylamine is also used as a surfactant because of its complex interaction with the metal ions to prevent the nanocrystals agglomeration, like oleic acid.

In a typical procedure, $ZnCl_2$ and the appropriate amount of $MnCl_2$ or $CuCl_2$ and $AlCl_3$ were first added to oleic acid (or dodecylamine) at room temperature. The resulting mixture was heated at 180 °C for 3 h to form the solution of zinc−oleic (or zinc−dodecylamine) complex. Then, elemental sulfur, which was dissolved in oleic acid or dodecylamine, was put into the resulting complex (the ratio between the total amount of salt and sulfur is controlled to be 1:3). The reactants were sealed in a 20-mL Teflon-lined autoclave and heated at 180 °C for 60 h. After the reaction was completed, the autoclave was taken out and allowed to cool to room temperature. The products were precipitated with ethanol, separated by centrifugation, and then dried at 60 °C for 1 h. To investigate the effect of posttreatment on the crystallinity and PL properties of nanospheres, part of the samples were annealed in the quartz tube under argon atmosphere at 600 °C for 1 h.

B. Preparation of ZnS Nanospheres with Core/Shell Structures. *1. Preparation of ZnS/SiO₂.* The ZnS/SiO_2 nanospheres were prepared by tetraethyl orthosilicate (TEOS) hydrolysis. Typically, an appropriate amount of ZnS nanospheres was dispersed in 80 mL of 2-propanol by sonicating for more than 30 min. Deionized water (7.5 mL) and 28% ammonia (9 mL) was added to keep the pH value at 8−9. Finally, the right amount of TEOS was added. The mixture was then placed for about 4 h at room temperature under vigorous stirring.

2. Preparation of ZnS/TiO₂. The ZnS/TiO_2 nanospheres were prepared by tetrabutyl titanate (TTBT) hydrolysis. Compared with TEOS, the hydrolysis rate of TTBT is very fast. Therefore, the required amount of water is very little. Typically, an appropriate amount of ZnS nanospheres was dispersed in 80 mL of 2-propanol by sonicating for more than 30 min. Then 28% ammonia (9 mL) was added to keep the pH value at 8−9, and later deionized water (7.5 mL) and the right amount of TTBT were added into the mixture drop by drop. The mixture was then placed for about 4 h at room temperature under vigorous stirring.

C. Property Characterizations of Doped and Coated ZnS Nanospheres. The XRD patterns of nanospheres were obtained on a Bruker D8 Advanced X-ray diffractometer with Cu−Kα radiation ($\lambda = 1.5418$ Å). The observation of the morphology and electron diffraction patterns were performed on a Hitachi Model 800 transmission electron microscope at acceleration voltage 200 kV. Samples for TEM were prepared by making clear dispersion of the nanocrystallites in hexane and putting drops of it on a carbon-coated copper grid. The EDS measurements were carried out on a JEOL JEM-2010 energy dispersive spectrometer. The optical absorption spectra of the nanospheres were measured using a Hitachi U-3010 UV−vis spectrophotometer. The optical absorption spectra were recorded from 200 to 600 nm at room temperature. The photoluminescence spectra were taken through a Hitachi Model F-4500 spectrofluorometer at room temperature.

Results and Discussions

1. Synthesis of Doped ZnS Nanospheres. In this report, a novel chemical route to well-crystallized ZnS nanospheres in homogeneous solution under easily controlled and mild conditions has been presented. In oleic acid or dodecylamine system, the probable effect on the growth of ZnS can be understood as the following equations:

$$Zn^{2+} + xRCO_2H \rightarrow [Zn(RCO_2H)_x]^{2+}$$

$$Zn^{2+} + xRH_2N \rightarrow [Zn(RH_2N)_x]^{2+}$$

Because of the coordination ability of the surfactant, they can interact with Zn^{2+} by coordination reaction to form surfactant−zinc complex. In other words, zinc ions are first separated from each other by the surfactant. Then, the independent nucleation and growth of each Zn^{2+} prevent the agglomeration of nanospheres. When oleic acid is used as surfactant, the addition of a small amount of triethylamine can improve the coordination ability of oleic acid for triethylamine is considered the catalyst.

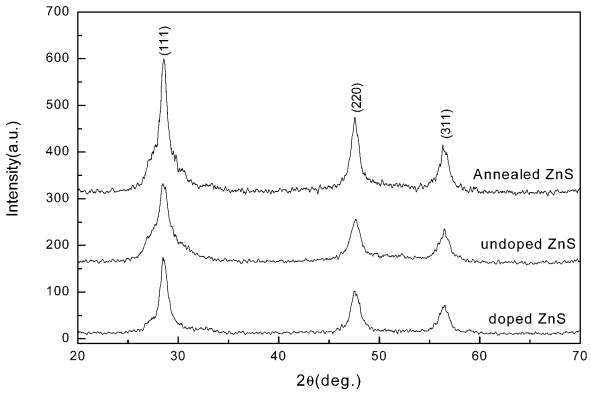

Figure 1. XRD patterns of ZnS nanospheres.

Powder XRD patterns of the various ZnS nanospheres are shown in Figure 1. The broad peaks in the XRD pattern compared to those of bulk ZnS indicate the nanocrystalline nature of the samples.

These diffraction features appearing at 28.5°, 47.5°, and 56.3° correspond to the (111), (220), and (311) planes of cubic zinc blende structure, which is very consistent with the values in the standard card (JCPDS No. 5-0566). The mean nanoparticle size of all samples estimated from the Debey−Scherrer formula[38] based on the full width at half-maximum of (111) zinc blende reflection is 10 nm, which shows that posttreatment has no effect on crystallite size but results in an increase in crystallinity of nanospheres. The similar XRD patterns of the pure and doped ZnS nanospheres reveal that doped ZnS still remains the crystal lattice of zinc blende.

2. Synthesis of Coated ZnS Nanospheres. Ströber et al. have developed a method in which SiO_2 particles can form by the hydrolysis and polycondensation of tetraethoxysilane under alkaline conditions in ethanol.[39] Since then, various approaches, inspired by Ströber's method, have been reported for the preparation of coated inorganic nanoparticels (such as Au, Ag,CdS, CdTe, CdSe, and CdSe/CdS).[40−44] The chemical process in the studied system can be described as

$$ZnS + Si(OC_2H_5)_4 + NH_3 + 4H_2O \rightarrow ZnS{-}SiO_2 + 4C_2H_5OH + NH_3$$

$$ZnS + Ti(OC_4H_9)_4 + NH_3 + 4H_2O \rightarrow ZnS{-}TiO_2 + 4C_4H_9OH + NH_3$$

A typical synthesis of silica-coated zinc sulfide nanospheres is described hereafter and schematically illustrated in Figure 2, which is the same for titania coating. First, ZnS nanospheres

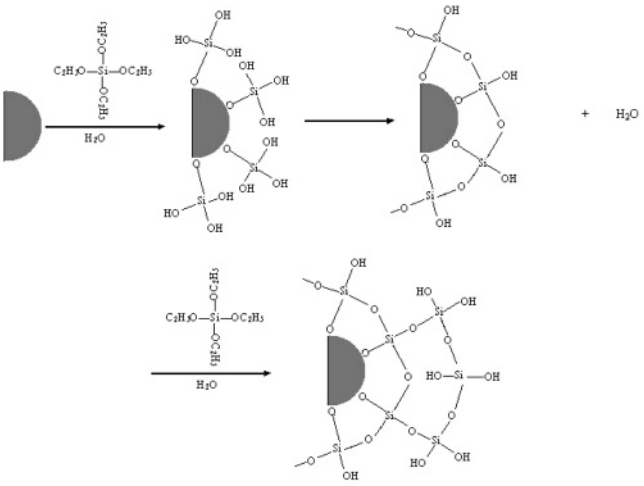

Figure 2. Schematic of the silinization method for ZnS nanospheres.

were dispersed into 2-propanol by sonicating to form a suspension. When TEOS was added, with the existence of water and ammonia, ethyloxysilane groups ($Si-OC_2H_5$) would hydrolyze into silanol groups (Si−OH). These silanol groups would adhere to the surface of nanospheres because of electrostatic forces. Then, the Zn^{2+} on the surface of nanospheres would react with silanol groups and build up Zn−O−Si bonds, which could enhance the adhesion of oxide coating on ZnS nanospheres by forming a primary polymerization layer. After heating, two adjacent silanol groups would form siloxane bonds through condensation reaction and release one water molecule. The left silanol groups acted as anchor points for subsequent silica shell growth. In this process, water plays a critical role since it drives the partial hydrolysis of the ethyloxysilane groups into silanols and allows a primary polymerization due to the hydrogen bonds between silanols.

The condition here chosen favors a very slow polymerization process around the nanospheres and minimizes an internanosphere cross-linking. Among these conditions, the temperature is an important factor. Mild temperature is helpful for the formation of van der Waals' force between silanol bridges (SiOH···HOSi), which will favor the later condensation reaction to form covalent siloxane bonds (−Si−O−Si−). Heating too violently or too long will cause the flocculation in the solution because it speeds up the polymerization rate of the silane reagents and induces internanosphere cross-linking. The heating temperature and time have been empirically determined in the experiments and can be varied over a broad range of values. To obtain nanospheres with perfect shell concerning the shell homogeneity, room temperature (about 20 °C) and reaction time of 4 h were chosen in our work.

3. Morphology of Nanospheres. Figure 3 shows the TEM images of doped ZnS nanospheres. From Figure 3a and b, it is observed that all the nanospheres are monodisperse and doped ions do not affect the morphology of nanospheres. These nanosphere have an average diameter of 100 nm. From the higher magnification TEM image (see Figure 3b), it can be seen that each nanosphere consists of many ultrafine particles with an average diameter of 10 nm, which is good agreement with the calculated results from XRD patterns. This kind of phenomena is observed too in CdS nanospheres.[45] The selected area electron diffraction (SAED) pattern in Figure 3c indicates that these nanospheres are of high crystalline. The three inside track diffraction rings correspond to the (111), (220), and (311) reflections of cubic ZnS, respectively, which is fully consistent

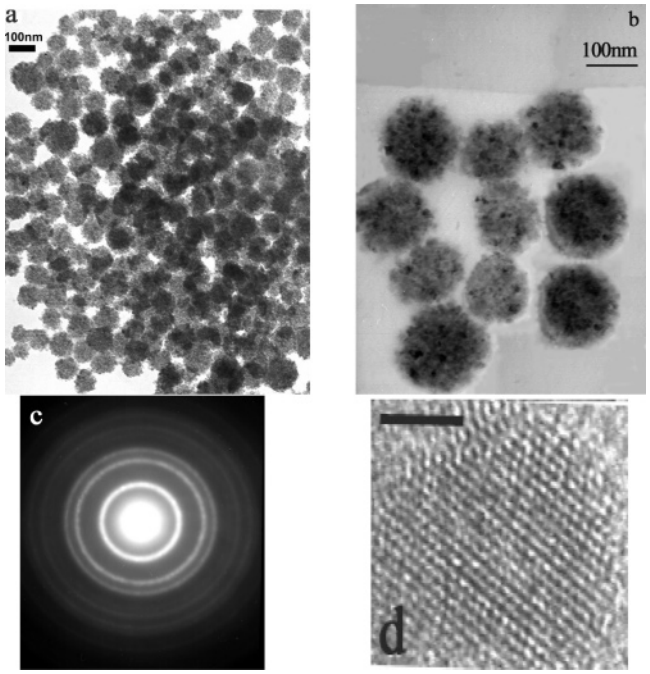

Figure 3. (a) Low magnification TEM images of doped ZnS nanospheres, (b) higher magnification TEM image of doped ZnS nanospheres, (c) SAED image, (d) HRTEM image (bar scale = 5 nm).

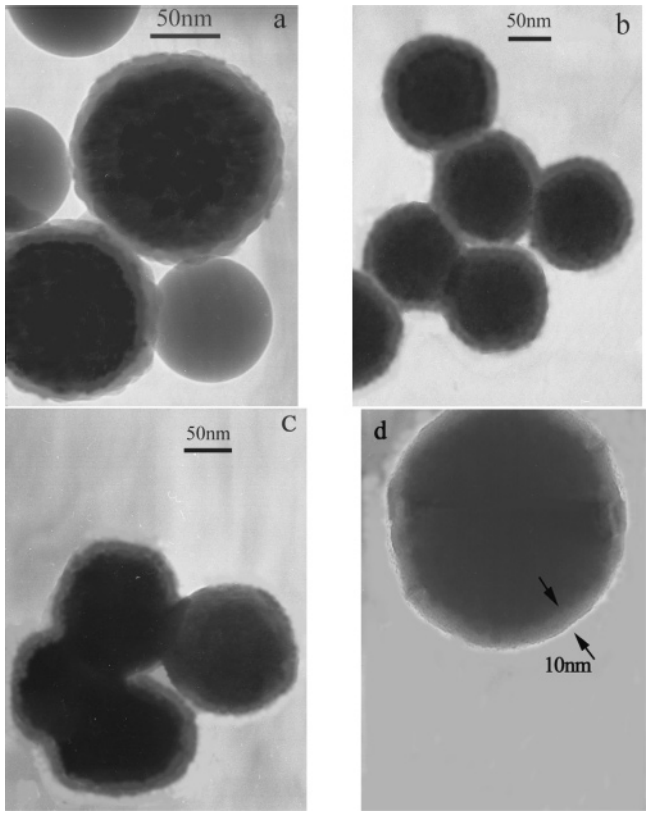

Figure 4. TEM images of coated ZnS nanospheres with different shell/core weight ratio. (a) Coated ZnS with high weight ratio (>1.0); (b) 0.68 SiO_2/ZnS weight ratio; (c) 0.6 TiO_2/ZnS weight ratio; (d) high magnification image of coated ZnS.

with the XRD results. The HRTEM image demonstrates well-resolved diffraction fringes of the particle lattices (in Figure 3d).

Table 1 summarizes a series of experiments carried out with different weight ratios of SiO_2 (TiO_2)/ZnS in solution. The weight ratio of SiO_2 (TiO_2) to ZnS is altered from about 0.6 to

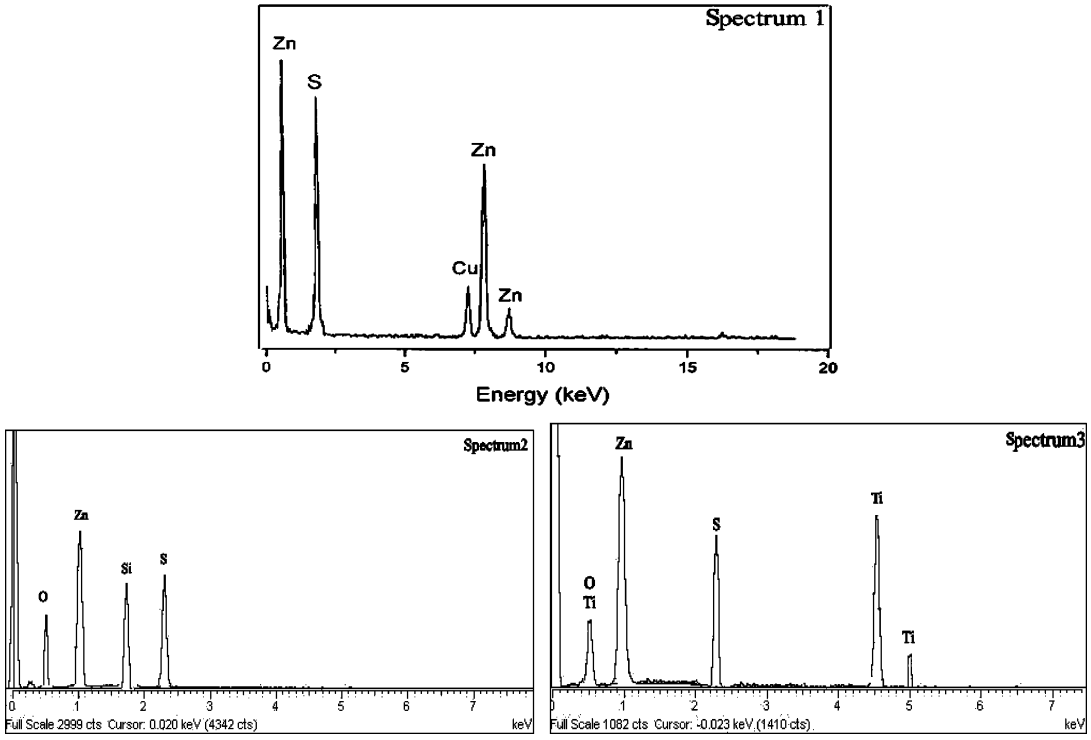

Figure 5. EDS patterns of the uncoated and coated ZnS nanospheres.

TABLE 1: Conditions for the Preparation of ZnS Nanoparticles Coated with Silica/Titania in 2-Propanol at Room Temperature for 4 h

sample no	TEOS (ml)	TBT (ml)	SiO_2/ZnS (wt %)	TiO_2/ZnS(wt %)
S1	1		6.8	
S2	0.6		4.08	
S3	0.4		2.72	
S4	0.2		1.36	
S5	0.1		0.68	
T1		1		6.0
T2		0.6		3.6
T3		0.4		2.4
T4		0.2		1.2
T5		0.1		0.6

6.8. The shell thickness could be adjusted by altering the concentration of cores and coating materials. To obtain well-dispersed coated nanospheres, it is essential to adjust the concentration of starting materials. The experiment results show that under identical conditions, the uniformity of the core/shell structures strongly depends on the exposed surface areas relative to the shell materials. If the amount of zinc sulfide cores is too small and the concentration of TEOS/TTBT is too high, mixtures of coated particles and silica/titania hydrous oxides are obtained.

Figure 4 shows the TEM images of coated ZnS nanospheres with different shell/core weight ratios. When the weight ratio is higher than 1.0, it is observed that mixtures of coated spheres and silica/titania hydrous oxides are obtained (see Figure 4a) in our experiments. In Figure 4a, small spheres are silicon dioxide and the large ones are coated ZnS nanospheres. Independent coated nanospheres can be obtained in suitable weight ratio ranges (0.60−1.0) (see Figure 4b, c). It can be observed that the spheres have a core−shell structure and the silica shell is clearly visible. It clearly indicated that silica-coated hybrid nanospheres are fairly well dispersed, regular spherical shape with an average diameter of about 120 nm. Each hybrid sphere is composed of two parts. The shell thickness is estimated to be about 10 nm. The cores are about 100 nm in diameter (see Figure 4d).

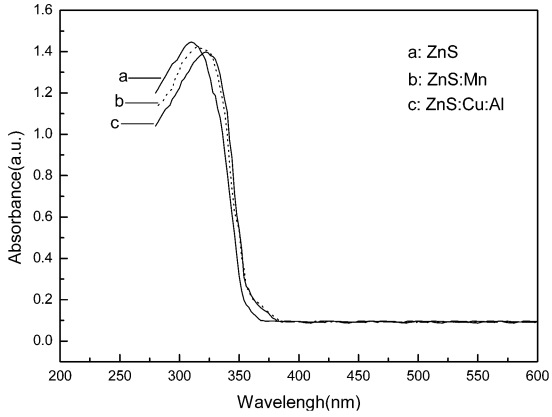

Figure 6. The absorption spectra of ZnS and doped ZnS nanospheres.

EDS analysis was performed on the coated samples to further characterize the surface of nanospheres. From spectrum 2 in Figure 5, it is clearly shown that Zn, S, O, and Si peaks are at their normal energies, which indicate that the coated layer is SiO_2. In like manner, the Zn, S, O, and Ti peaks in spectrum 3 indicate the formation of TiO_2 layers. No Si or Ti peak can be found in spectrum 1 of the bare particles. Therefore, on the basis of the results of EDS and TEM, we can confirm the complete encapsulation of ZnS nanospheres by uniform nanoscale layers.

4. The Absorption Spectra and PL Spectra of Nanospheres. Figure 6 shows the UV−vis absorption spectra of both the pure and doped ZnS nanospheres. These spectra are structured with the absorption maximum at 310 nm (ZnS), 315 nm (ZnS:Mn), and 320 nm (ZnS:Cu:Al), respectively, which are distinctly different to the bulk ZnS (at ∼340 nm).

This absorption in the spectra corresponds to the $1S_e-1S_h$ excitation transitions of the nanospheres. The onset of absorption shifts toward shorter wavelength from doped ZnS to pure ZnS, which demonstrates the change of energy band gap in the nanospheres. The absorption onset will shift to high energy with the nanoparticle size decreasing. From the TEM images, we

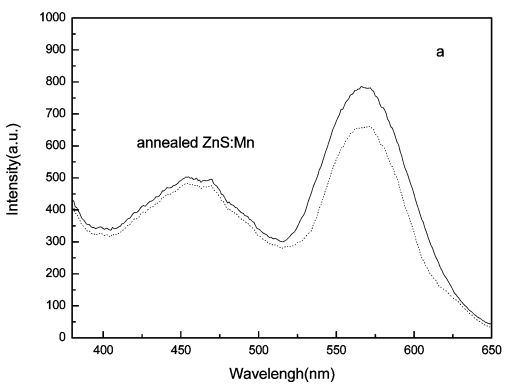

Figure 7. PL spectra of doped ZnS nanospheres.

can find that the pure and the doped ZnS nanospheres have the same particle size. Therefore, the shift of the absorption onset cannot be attributed to the particle size but to the doped ions. Two factors may be responsible for the redshift of the band gap. One is the possible formation of Zn−metal−S ternary system solid solution. For doped ZnS nanospheres, metal ions will occupy the Zn^{2+} sites in the lattice and will lead to the formation of Zn−metal−S ternary system, whose band gap will be determined by the ratio of Zn and metal ions. Despite the small amount of doped ions in the ZnS nanospheres, the energy band of doped ZnS changes with different doped ions. The other possible explanation may be related to the electronic population of doping at band edge.

The PL spectra of doped ZnS nanospheres are shown in Figure 7, which exhibit that all the spectra are Gaussian distribution. Figure 7a shows the PL spectrum of ZnS:Mn nanospheres for 320-nm excitation, which exhibits two broad emission bands. The strongest peak with the maximum around 572 nm (orange) is attributed to the $^4T_1-^6A_1$ transition with the $3d^5$ configuration of the Mn^{2+} ion.[46−47] The higher energy with the maximum around 450 nm belongs to a violet defected related which is assigned to recombination at sulfur vacancies in the materials. It is also observed in undoped ZnS nanospheres. The emission spectra of ZnS:Cu:Al nanospheres display the green emission (see Figure 7b) located at 530 nm (green) which originated from the radiative energy relaxation between trapped activator level within the band gap and the valence band edge, corresponding to the transition of $3d^{10}$ to the transition of $3d^{10}$ to $3d^94s^1$ at those interstitial Cu^+ centers.

For comparison with nonannealed nanospheres, annealed nanospheres exhibit stronger PL properties (see solid line in Figure 7a, b) at the same measurement condition. These results of PL spectra are consistent with those of XRD, which indicate that the particles with better crystallinity have higher PL intensities than those of poor crystallinity. Generally, the PL properties of particles are impacted by many factors, such as particle shape, size, size distribution, and so on. In particular, the effect of particle crystallinity could not be ignored. It is thought that nanospheres with higher crystallinity have low concentration of defects, which act as sites for nonradiative recombination of electron−hole pairs. As a result, the emission intensities can be enhanced. Therefore, posttreatment has an effect on improving the brightness of nanospheres.

Figure 8 gives the PL spectra of silica/titania coated and uncoated ZnS. It is quite interesting as there is no shift in the luminescence peak position, but the intensity changes are prominent. Compared with uncoated ZnS, the emission spectra of coated ZnS are narrow and symmetric. Full width at half-maximum (fwhm) values of 50 nm is obtained. We interpret

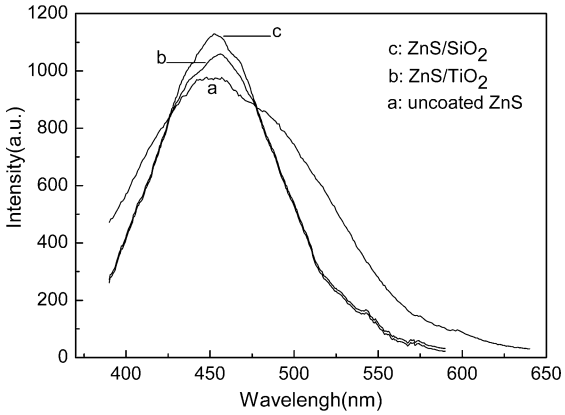

Figure 8. PL spectra of coated and uncoated ZnS nanospheres.

this enhancement of the photoluminescence intensity as removal of electron capture centers on the surface of ZnS nanospheres or removal of nonradiative decay channels because of the silica/titanium shell around ZnS nanospheres. Moreover, we cannot exclude the presence of the nanospheres agglomeration during many purification steps. As a result, coating can also reduce phosphor surface degradation associated with display fabrication process, thus reducing the surface dead later thickness and passivating surface recombination centers.

5. The Thermal Stability of Nanospheres. As mentioned previously, coating is expected to reduce phosphor surface degradation (such as oxidation) association with display fabrication process. To investigate the thermal stability after coating, coated and uncoated phosphors were heated simultaneously to 300, 400, 500, 600, and 700 °C for 1 h in air. Then, PL measurement was performed to evaluate the degree of thermal degradation of coated and uncoated phosphors. Figure 9 shows the normalized PL intensity as a function of firing temperature under same excitation.

As shown, the coated samples maintained the original efficiency up to 600 °C before suffering a moderate decrease at 700 °C. The uncoated samples, on the other hand, show a continuous gradual decrease. After heat treatment at 700 °C for 1 h in air, the PL intensities were 80% of their original values for the coated sample while for the uncoated sample PL intensity decreases to zero after heat treatment at 500 °C.

Figure 10 gives XRD patterns of the coated and uncoated sample after heat treatment at 500 °C in air. From the figure, it can be seen that after heat treatment at 500 °C in air, the silica coating sample still show the peaks of ZnS phosphors (because silica layer is amorphous it does not show any peaks in XRD pattern of coated particles). Titania coating sample shows the

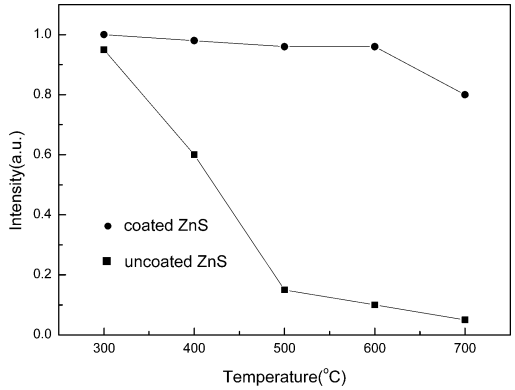

Figure 9. PL intensity of the coated and uncoaed ZnS as a function of firing temperature.

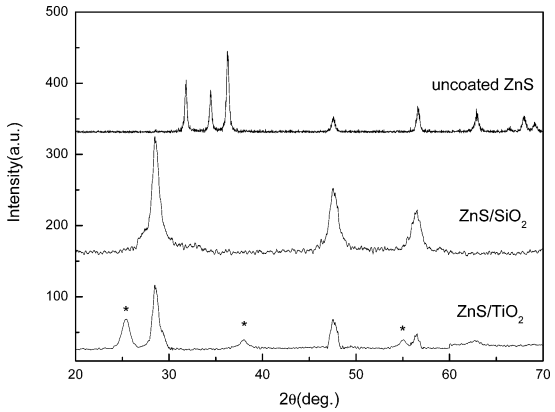

Figure 10. 10. XRD patterns of the uncoated and coated ZnS after heat treatment at 500 °C in air.

peaks of ZnS and TiO_2 (∗ is XRD peaks of TiO_2). The uncoated sample shows the peaks of ZnO because zinc sulfide decomposes in air above 500 °C. ZnO has no luminescence at measurement range. Therefore, it can be concluded that the coating protects the phosphors surface by prohibiting further stability of phosphors, which is critically important for FED panel manufacture.

Conclusions

In summary, highly monodisperse ZnS:Mn and ZnS:Cu:Al nanospheres with an average diameter of 100 nm were synthesized by a solvothermal route, which is an easily controllable, safe, and convenient route. The tunable, symmetric photoluminescence emissions were achieved by metal ions doped ZnS nanospheres. It is possible to extend this approach to the formation of other monodisperse transition-metal sulfides. Because this kind of ZnS is spherical and monodisperse, it is promising to satisfy the requirement for the future display technique development, such as flat screens, low operating voltage, high-resolution, and so forth. Uniform $SiO_2(TiO_2)$ coated ZnS nanospheres were successfully prepared by controlling the starting concentration of TEOS(TTBT) using the sol−gel technology. EDS and TEM confirmed the formation of thin and uniform coatings of ZnS nanospheres with thickness of 10−15 nm. PL spectrum of coated ZnS nanospheres show more narrow emission peak and higher intensity because of decreasing nonradiative centers and good dispersion. PL intensity remains unchanged after heat treatment at 500 °C by firing test indicating that coating layers protect the surface of ZnS nanospheres.

Acknowledgment. This work was supported by NSFC (50372030, 20025102, 20151001), the Foundation for the Author of National Excellent Doctoral Dissertation of P. R. China, and the state key project of fundamental research for nanomaterials and nanostructures (2003CB716901).

References and Notes

(1) Chen, W.; Joly, A. G.; Zhang, J. Z. *Phys. Rev. B* **2001**, *64*, 41202.
(2) Yang, H. S.; Holloway, P. H.; Ratna, B. B. *J. Appl. Phys.* **2003**, *93*, 586.
(3) Do, Y. R.; Kim, Y. C.; Cho, S. H.; Ahn, J. H.; Lee, J. G. *Appl. Phys. Lett.* **2003**, *82*, 4172.
(4) Xu, C. N.; Watanabe, T.; Akiyana, M.; Zheng, X. G. *Mater. Res. Bull.* **1999**, *34*, 1491.
(5) Chen, W.; Wang, Z.; Lin, Z. *Appl. Phys. Lett.* **1997**, *70*, 1465.
(6) Bredol, M.; Merichi, J. *J. Mater. Sci.* **1998**, *33*, 471.
(7) Calandra, P.; Gofferdi, M.; Liveri, V. T. *Colloids Surf., A* **1999**, *9*, 160.
(8) Prevenslik, T. V. *J. Lumin.* **2000**, *87*, 1210.
(9) Bulanyi, M. F.; Kovalenko, A. V.; Polezhaev, B. A. *Inorg. Mater.* **2000**, *39*, 222.
(10) Khosravi, A. A.; Kundu, M.; Jatwa, L.; Desphpande, S. K.; Bhagwat, U. A.; Sastry, M.; Kulkarni, S. K. *Appl. Phys. Lett.* **1995**, *67*, 2702.
(11) Yang, P.; Lu, M.; Xu, D.; Yuan, D.; Song, C.; Zhou, G. *J. Phys. Chem.* **2001**, *62*, 1181.
(12) Xu, S. J.; Chua, D. J.; Liu, B.; Gan, L. M.; Chew, C. H.; Xu, G. Q. *Appl. Phys. Lett.* **1998**, *73*, 478.
(13) Kim, J. P.; Davodson, M. R.; Holloway, P. H. *J. Appl. Phys.* **2003**, *93*, 9597.
(14) Wang, Y. J.; Wu, C. X.; Chen, M. Z.; Huang, M. C. *J. Appl. Phys.* **2003**, *93*, 9625.
(15) Kang, Y. C.; Park, S. B.; Lenggoro, I. W.; Okuyama, K. *J. Phys. Chem. Solids* **1999**, *60*, 379.
(16) Li, Q.; Wang, C. R. *Appl. Phys. Lett.* **2003**, *83*, 359.
(17) Meng, X. M.; Jiang, Y.; Liu, J.; Lee, C. S.; Bello, I. *Appl. Phys. Lett.* **2003**, *83*, 2244.
(18) Jiang, Y.; Meng, X. M.; Liu, J.; Hong, Z. R.; Lee, C. S.; Lee, S. T. *Adv. Mater.* **2003**, *15*, 1195.
(19) Zhao, Q.; Hou, L. S.; Huang, R. A. *Inorg. Chem. Commun.* **2003**, *6*, 971.
(20) Xia, Y. N.; Gates, B.; Yin, Y. D.; Lu, Y. *Adv. Mater.* **2000**, *12*, 693.
(21) Deng, Z. X.; Wang, C.; Sun, X. M.; Li, Y. D. *Inorg. Chem.* **2002**, *41*, 869.
(22) Heng, R.; Qian, X. F.; Yin, J.; Xi, H. A.; Bian, L. J. *Colloids Surf., A* **2003**, *220*, 151.
(23) Ohko, Y.; Setani, M.; Sakata, T.; Mori, H.; Yoneyama, H. *Chem. Lett.* **1999**, *7*, 663.
(24) Miyoshi, H.; Mori, H.; Yoneyama, H. *Langmuir* **1991**, *7*, 503.
(25) Abe, T.; Tachibana, Y.; Vematsu, T.; Twamoto, M. *Chem. Commun.* **1995**, 1617.
(26) Dabbousi, B. O.; Rodriguez-Viejo, J.; Mikulec, F. V.; Haeine, J. R.; Mattoussi, A. *J. Phys. Chem. B* **1997**, *101*, 9463.
(27) Peng, X.; Schlamp, M. C.; Kadavanich, A. V.; Alivisatos, A. P. *J. Am. Chem. Soc.* **1997**, *119*, 7019.
(28) Lu, S. Y.; Wu, M. L.; Chen, H. L. *J. Appl. Phys.* **2003**, *93*, 5789.
(29) Gerion, D.; Pinaud, F.; Williams, S. C.; Park, W. J. *J. Phys. Chem. B* **2001**, *105*, 8861.
(30) Hines, M. A.; Guyo-Sionnest, Ph. *J. Phys. Chem.* **1996**, *100*, 468.
(31) Hasselbarth, A.; Eychmuller, A.; Eichberger, R.; Giersig, M. *J. Phys. C* **1993**, *97*, 5333.
(32) Do, Y. R.; Park, D. H.; Yang, H. G.; Park, W.; Wagner, B. K.; Yasuda, K.; Summers, C. J. *J. Electrochem. Soc.* **2001**, *148*, G581.
(33) Feldmann, C.; Merikhi, J. *J. Colloid Surf. Sci.* **2000**, *223*, 229.
(34) Merikhi, J.; Feldmann, C. *J. Colloid Surf. Sci.* **2000**, *228*, 121.
(35) Villalobos, R. G.; Bayya, S. S.; Sanghera, J. S.; Miklos, R. E. *J. Am. Ceram. Soc.* **2002**, *85*, 2128.
(36) Joo, J.; Na, H. B.; Yu, T.; Yu, J. H.; Kim, Y. W.; Wu, F. X.; Zhang, J. Z.; Hyeon, T. *J. Am. Chem. Soc.* **2003**, *125*, 11100.
(37) Zhang, Y.; Peng, Q.; Wang, X.; Li, Y. D. *Chem. Lett.* **2004**, in press.
(38) Guinier, A.; Freeman, W. H. X-ray Diffraction, San Francisco, CA, 1963.
(39) Stöber, W.; Frink, A.; Bohn, E. *J. Colloid Surf. Sci.* **1966**, *26*, 62.
(40) Correa-Duarte, M. A.; Giersig, M.; Liz-Marzan, L. M. *Chem. Phys. Lett.* **1998**, *286*, 497.
(41) Rogach, A. L.; Dattatri, N.; Ostrander, J. W.; Giersig, M.; Kotov, N. A. *Chem. Mater.* **2000**, *9*, 2676.
(42) Mulvaney, P.; Liz-Marzan, L. M.; Giersig, M.; Ung, T. *J. Mater. Chem.* **2000**, *10*, 1259.

(43) Liz-Marzan, L. M.; Giersig, M.; Mulvaney, P. *Langmuir* **1996**, *12*, 4329.
(44) Ung, T.; Liz-Marzan, L. M.; Mulvaney, P. *Langmuir* **1998**, *14*, 3740.
(45) Yao, H.; Takada, Y.; Kitamura, N. *Langmuir* **1998**, *14*, 595.
(46) Gan, L. M.; Liu, B.; Chew, C. H. *Langmuir* **1997**, *13*, 6427.
(47) Yu, I.; Isobe, T.; Senna, M. *J. Phys. Chem. Solids* **1996**, *57*, 373.